Supporting information for

Content (10 Pages)

Supplementary Figures S1–S9

Supplementary Tables S10

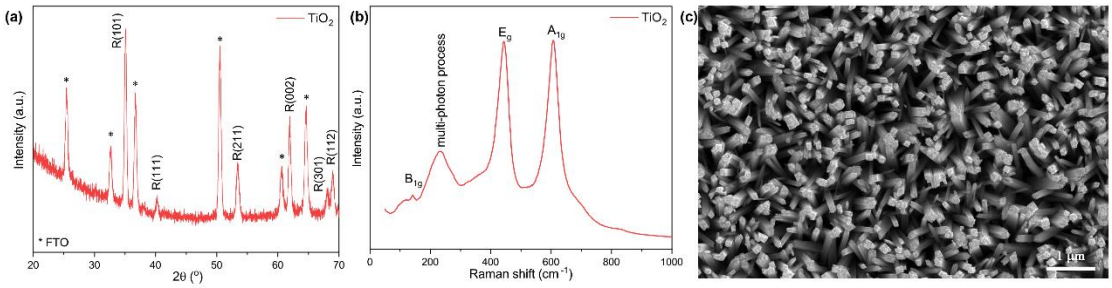

Figure S1. (a) XRD pattern, (b) Raman spectrum, and (c) SEM image of TiO_2 nanorod arrays film on FTO glass.

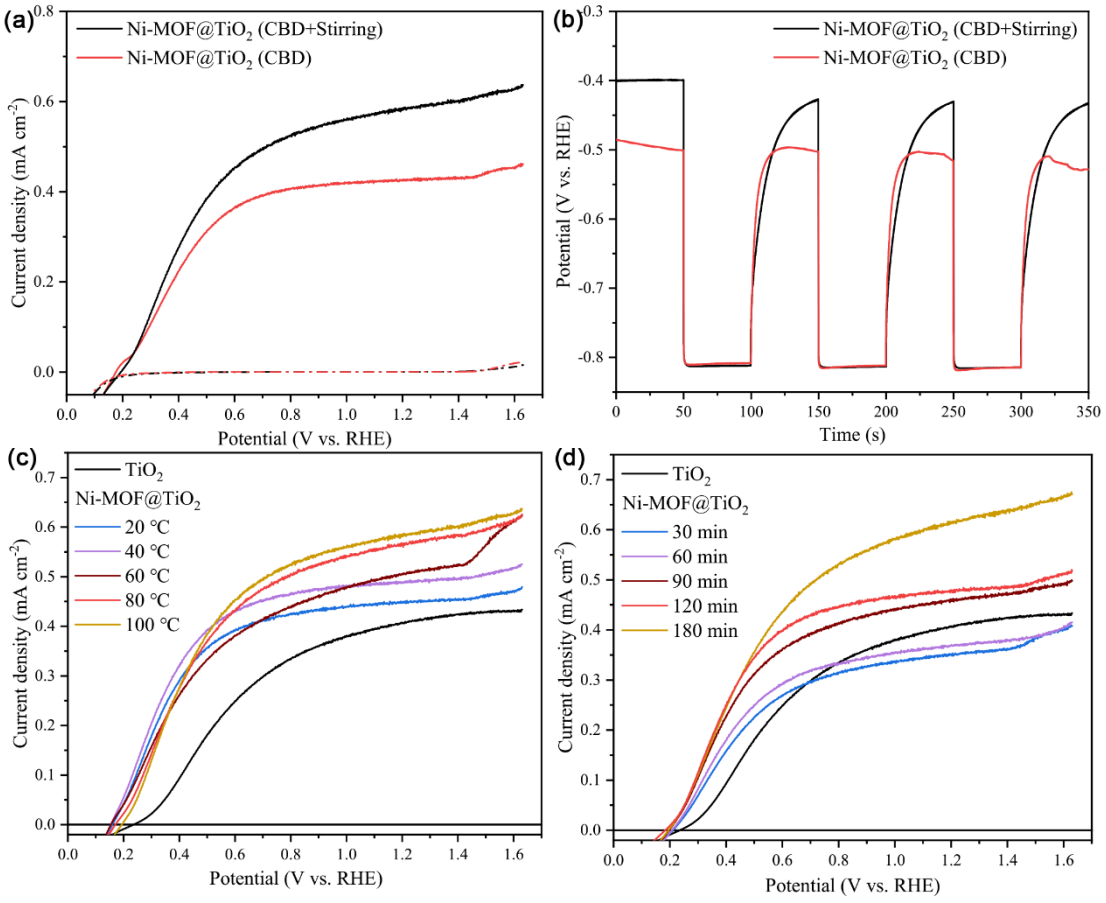

Figure S2. (a) LSV curves and (b) chopped OCP curves of Ni-MOF@TiO_2 prepared through CBD method with/without stirring. (c) LSV curves of Ni-MOF@TiO_2 prepared at different temperatures. (d) LSV curves of Ni-MOF@TiO_2 prepared with various times. The electrolyte is 1 M KOH/0.33 M urea.

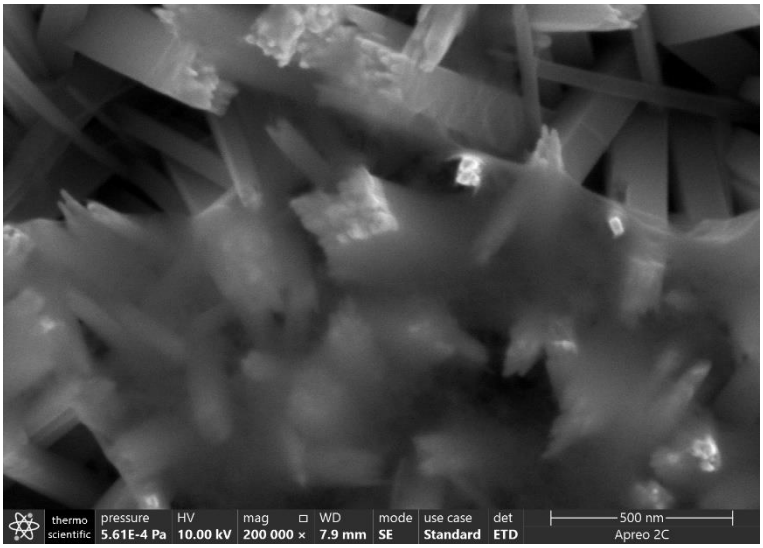

Figure S3. SEM image of Ni-MOF@TiO_2 film.

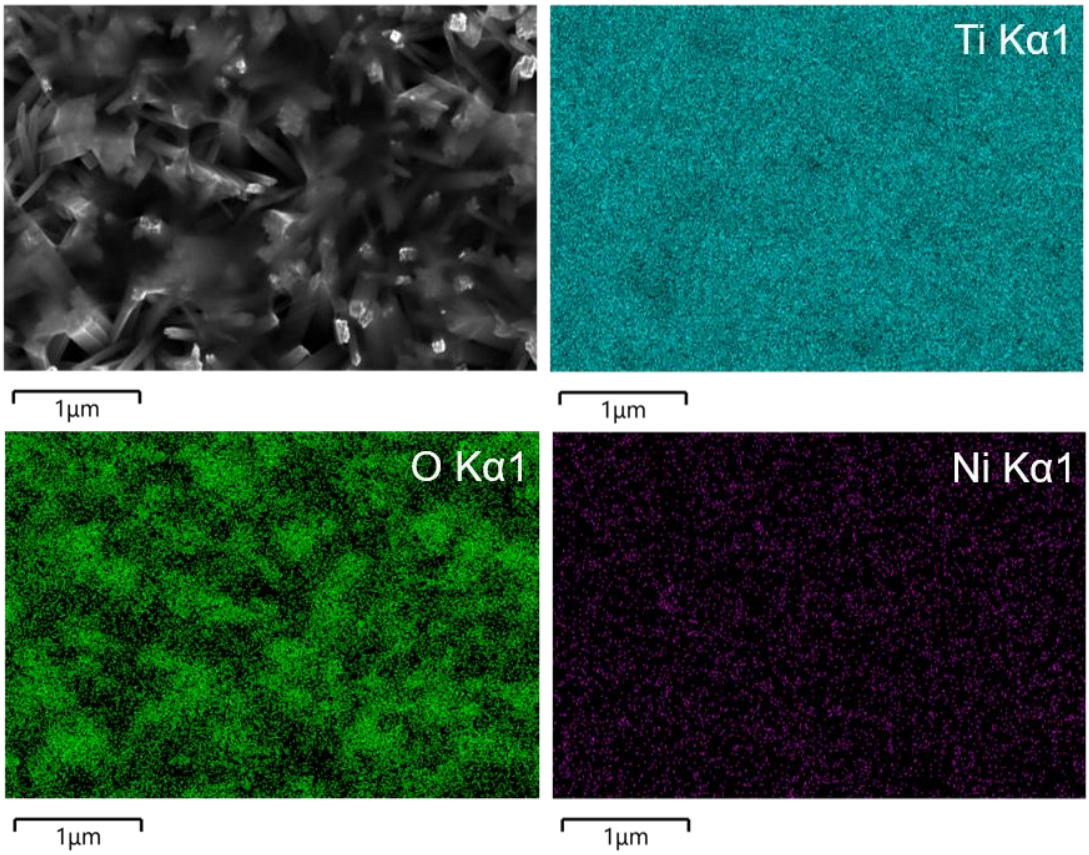

Figure S4. EDS mapping of T-$Ni(OH)_2$@TiO_2 film.

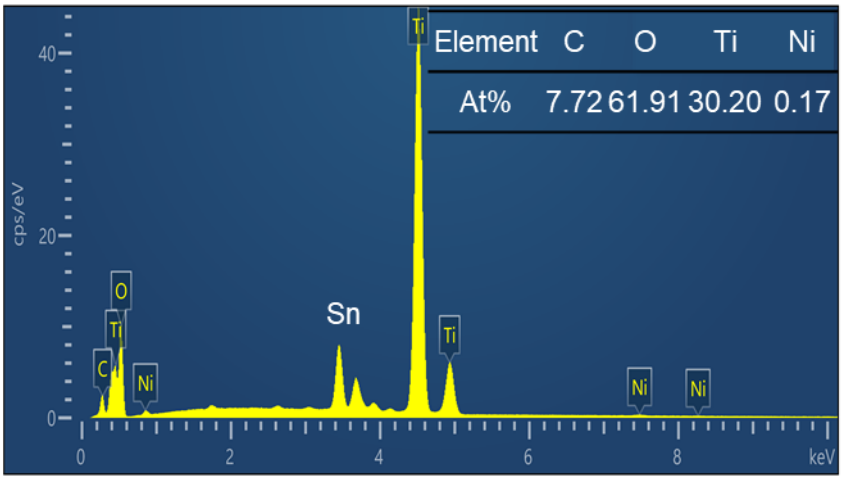

Figure S5. EDS pattern of T-Ni(OH)$_2$@TiO$_2$ film on FTO glass.

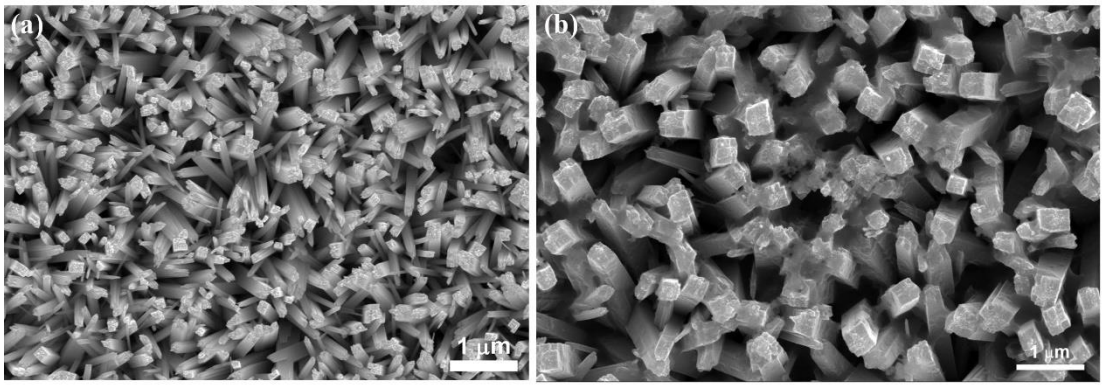

Figure S6. Top-view SEM images of (a) pristine TiO$_2$ and (b) Ni(OH)$_2$@TiO$_2$ films.

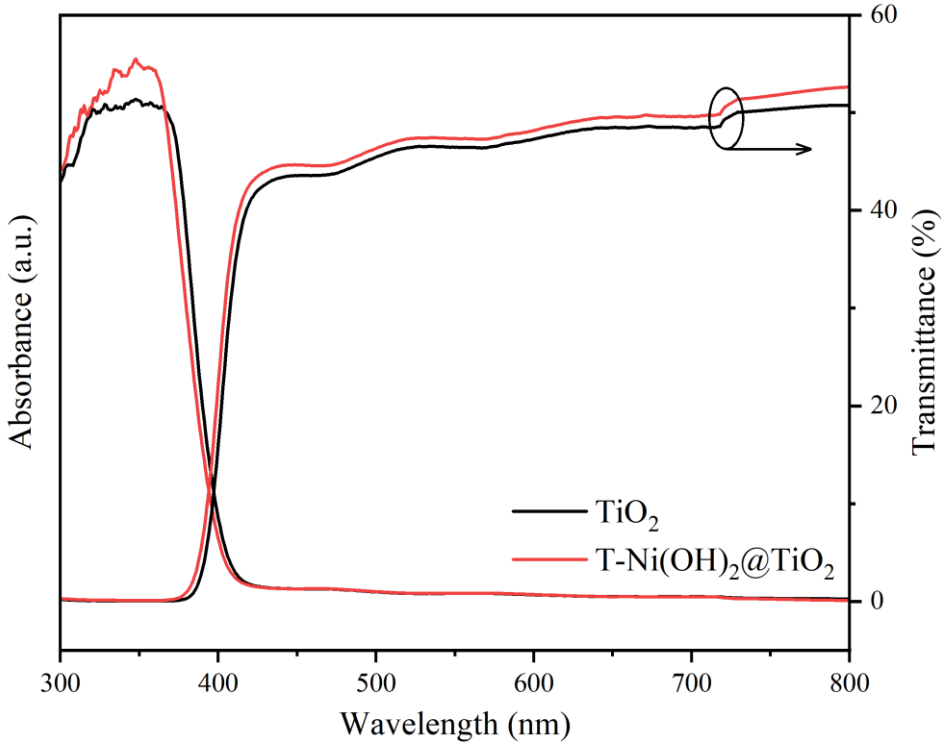

Figure S7. UV-vis absorption and transmittance spectra of TiO$_2$ and T-Ni(OH)$_2$@TiO$_2$ with 6 h EL

treatment.

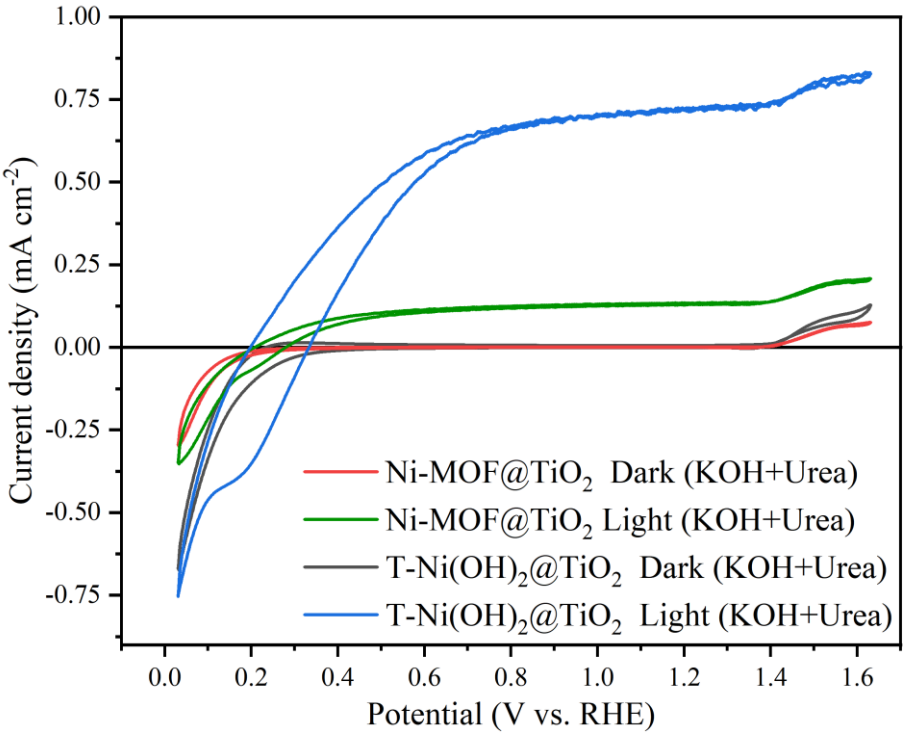

Figure S8. CV curves of Ni-MOF@TiO_2 and T-Ni$(OH)_2$@TiO_2 photoanodes with 1 h EL treatments under AM1.5G illumination and in the dark. Electrolyte: 1.0 M KOH and 0.33 M urea. Scan rate: 20 mV s^{-1}.

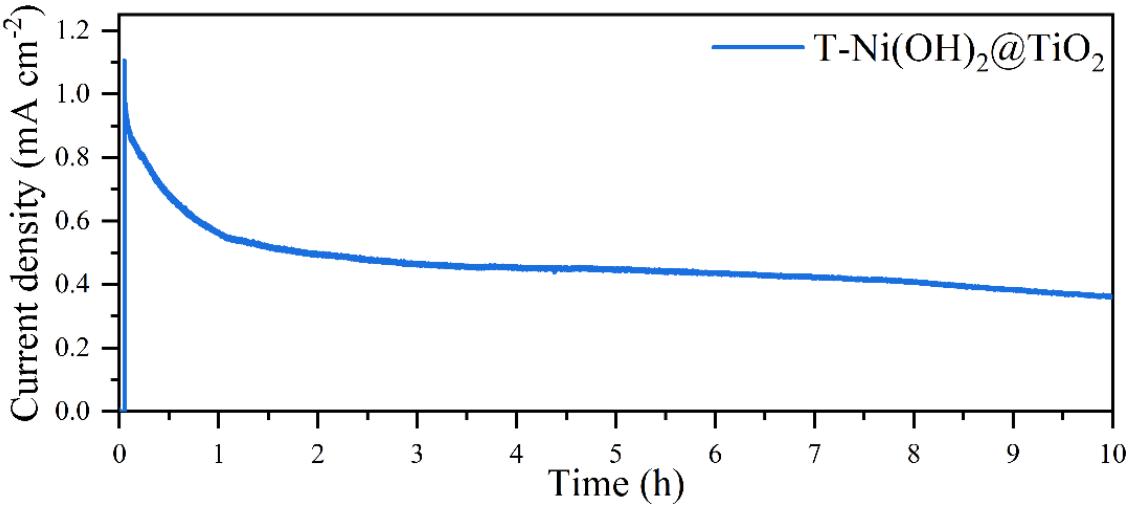

Figure S9. Long-term stability of T-Ni$(OH)_2$@TiO_2 photoanode at 1.23 V_{RHE} under AM1.5G illumination.

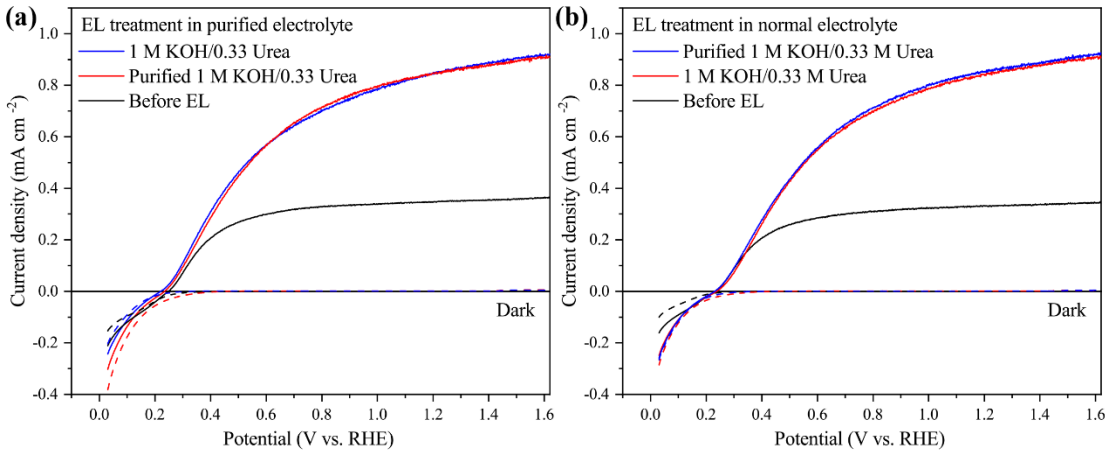

Figure S10. (a) LSV curves of T-Ni(OH)$_2$@TiO$_2$ photoanode with 1 h EL treatment in purified electrolyte. (b) LSV curves of T-Ni(OH)$_2$@TiO$_2$ photoanode with 1 h EL treatment in normal electrolyte. Scan rate: 20 mV s^{-1}. Illumination: AM1.5G illumination.

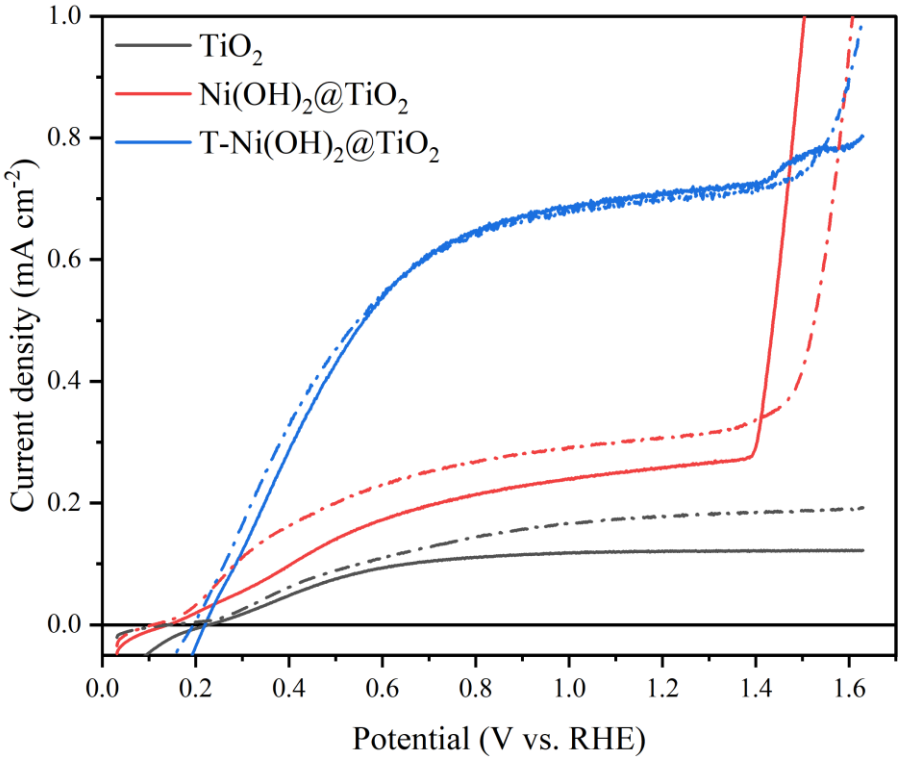

Figure S11. LSV curves of TiO$_2$, Ni(OH)$_2$@TiO$_2$, and T-Ni(OH)$_2$@TiO$_2$ photoanodes measured in 1 M KOH/0.33 M urea (Solid line) and 1 M KOH/0.33 M urea containing 0.5 M Na$_2$SO$_3$ (Dash line).

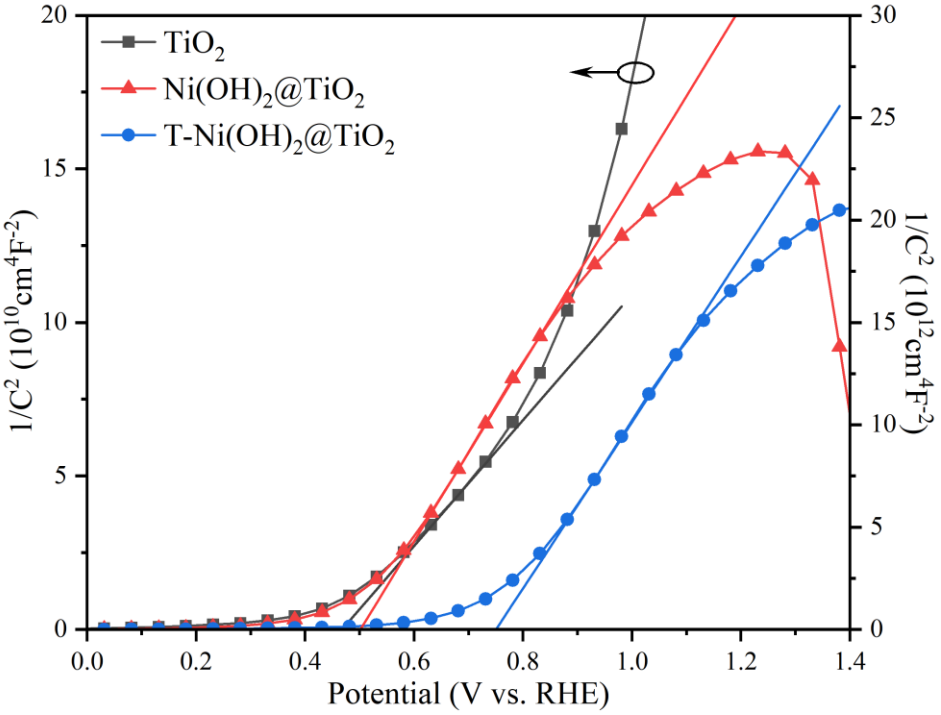

Figure S12. MS plots of TiO_2, $Ni(OH)_2@TiO_2$, and $T\text{-}Ni(OH)_2@TiO_2$ photoanodes measured at a fixed frequency of 1000 Hz in the dark.

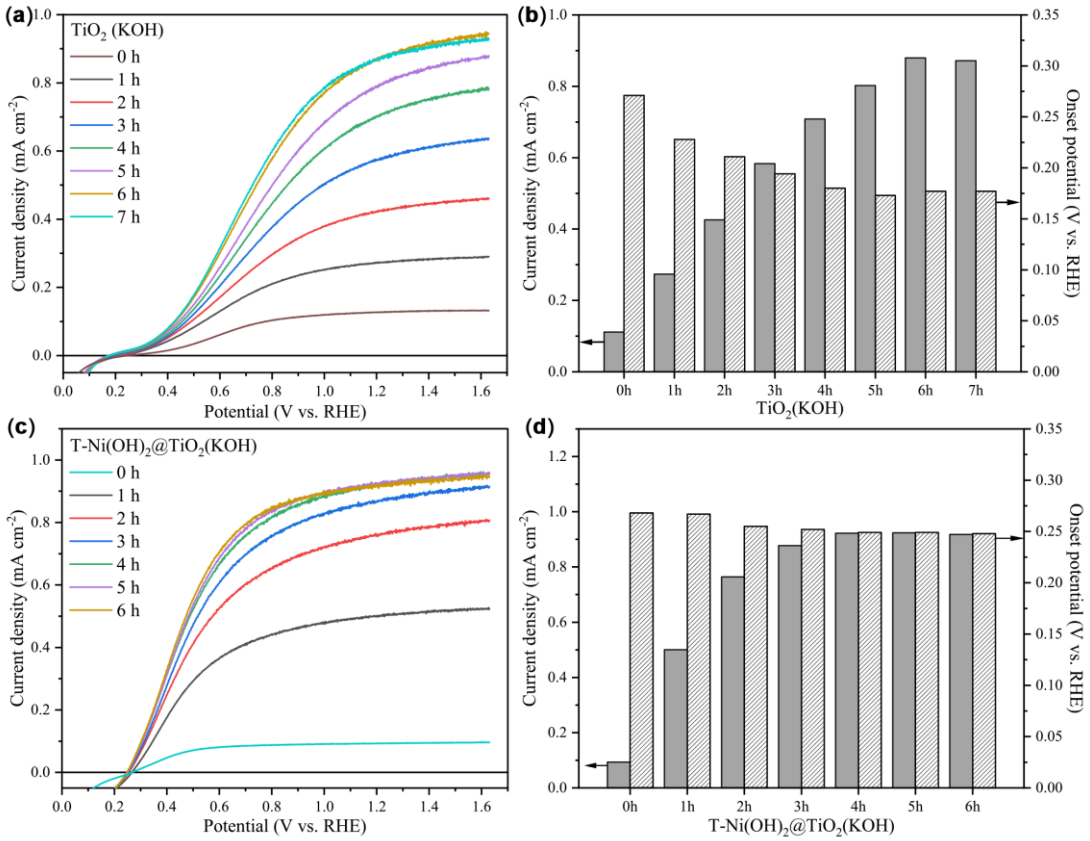

Figure S13. (a) LSV curves of TiO_2 after EL treatment with various times. (b) Histogram of

photocurrent density and onset potential of the above TiO_2 photoanodes. (c) LSV curves of T-$Ni(OH)_2$@TiO_2 after EL treatment with different times. (d) Histogram of photocurrent density and onset potential of the above T-$Ni(OH)_2$@TiO_2 photoanodes. Electrolyte: 1 M KOH. Light illumination: AM1.5G illumination. Scan rate: 20 mV s^{-1}.

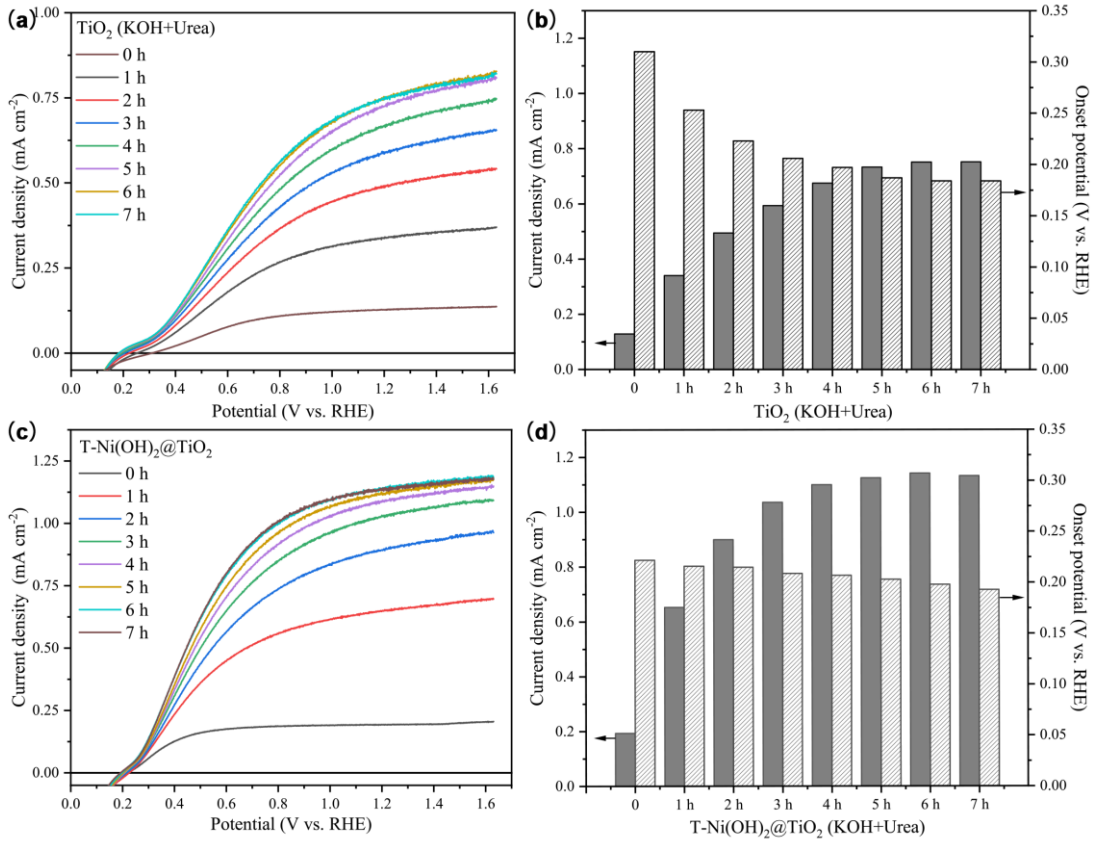

Figure S14. (a) LSV curves of TiO_2 after EL treatment with various times. (b) Histogram of photocurrent density and onset potential of the above TiO_2 photoanodes. (c) LSV curves of T-$Ni(OH_2)$@TiO_2 after EL treatment with different times. (d) Histogram of photocurrent density and onset potential of the above T-$Ni(OH_2)$@TiO_2 photoanodes. Electrolyte: 1 M KOH/0.33 M urea. Light illumination: AM1.5G illumination. Scan rate: 20 mV s^{-1}.

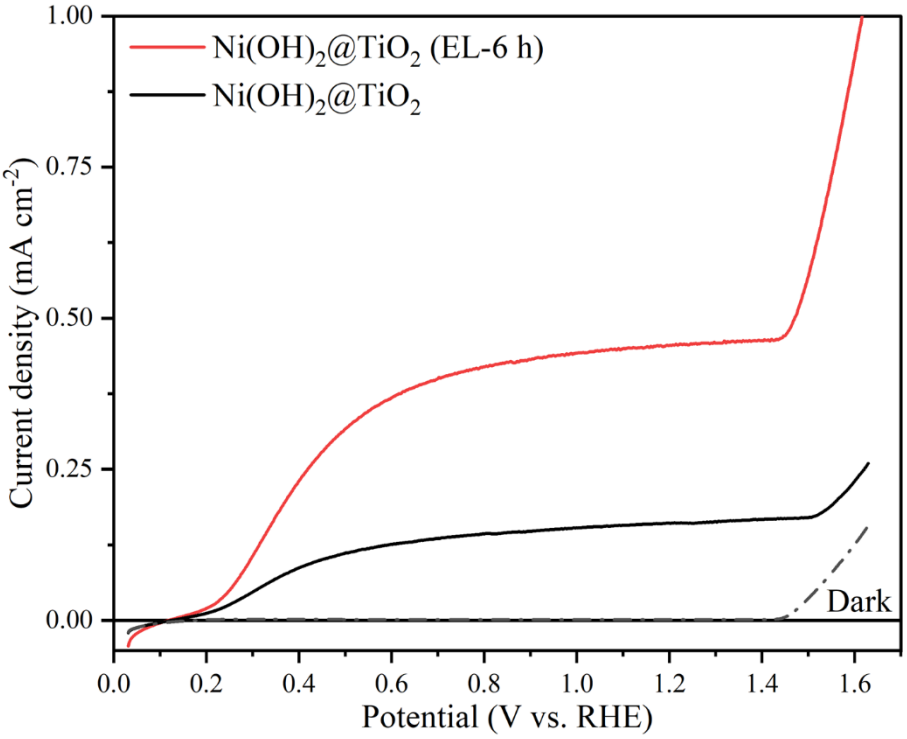

Figure S15. LSV curves of $Ni(OH)_2@TiO_2$ photoanode with/without EL treatment of 6 h. Electrolyte: 1 M KOH/0.33 M urea. Light illumination: AM1.5G illumination. Scan rate: 20 mV s^{-1}.

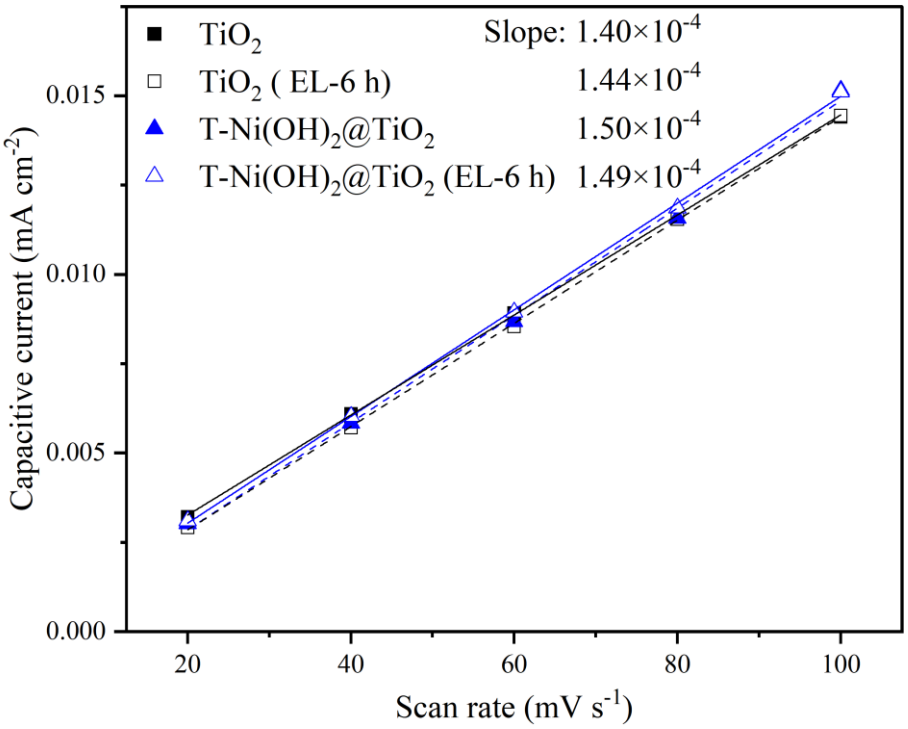

Figure S16. The relationship curves between the capacitance current and the scan rate of TiO_2 based photoanodes.

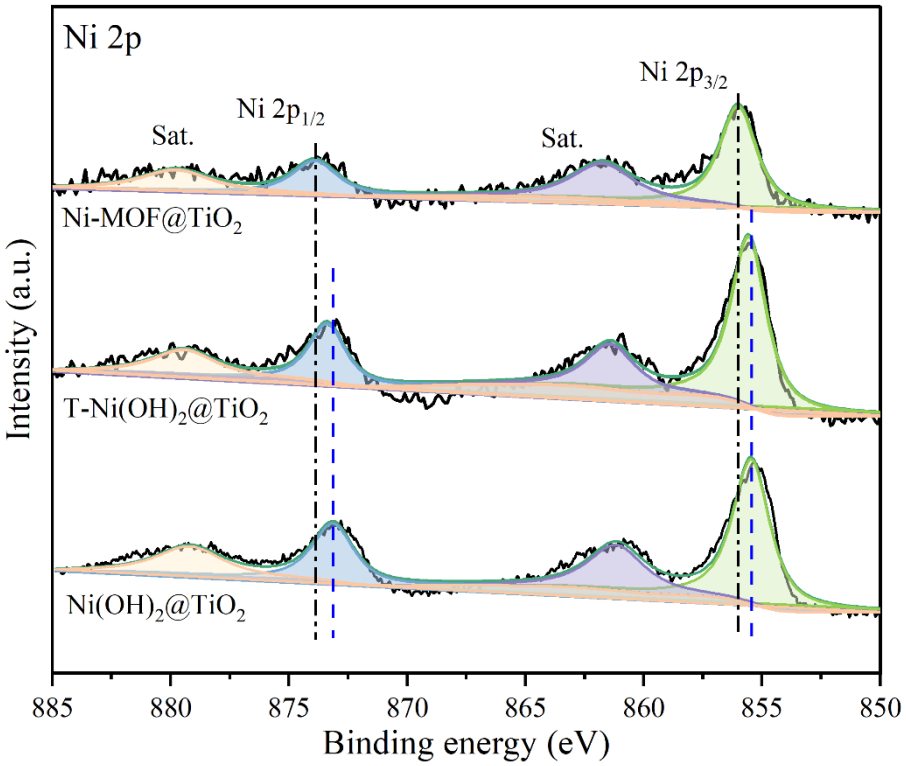

Figure S17. Ni 2p XPS spectra of Ni-MOF@TiO_2, T-$Ni(OH)_2$@TiO_2 and $Ni(OH)_2$@TiO_2.

Supplementary Tables

Table S1. PEIS fitting parameters of TiO_2, $Ni(OH)_2@TiO_2$ and T-$Ni(OH)_2@TiO_2$ photoanodes.

Photoanode	R_s (Ω)	R_{bulk} (Ω)	CPE_{bulk} (F)	R_{ct} (kΩ)	CPE_{ct} (F)
TiO_2	23.35	/	/	45.37	2.29E-5
$Ni(OH)_2@TiO_2$	9.47	1727.00	3.33E-6	28.54	4.05E-6
T-$Ni(OH)_2@TiO_2$	10.72	569.90	1.64E-6	15.58	2.75E-6